PCCP



PAPER View Article Online



Cite this: Phys. Chem. Chem. Phys., 2024, 26, 21030

complexes vs. irreversible reactions of anions with tetracyanoethylene†

Anion $-\pi$ interaction with alkenes: persistent

Favour E. Odubo, a Snehashree Muthuramesh, a Matthias Zeller and Sergiy V. Rosokha **

The interaction of the tetracyanoethylene (TCNE) π -acceptor with oxo- and fluoro-anions (BF₄ $^-$, PF₆ $^-$, ClO_4^- , NO_3^-) led to the formation of anion- π complexes in which these polyatomic anions were located over the face of alkenes, with multiple contacts being shorter than the van der Waals separations. The anion- π associations of TCNE with halides were delimited by the electron-donor strengths and nucleophilicity of the anions. Specifically, while bromides formed persistent anion- π associations with TCNE in the solid state and in solutions, only transient anion- π complexes with iodides and chlorides were observed. In the case of iodide (strong 1e reducing agent), the formation of anion- π complexes was followed by the reduction of the π -acceptor to the TCNE $^{-\bullet}$ anion-radical. The interaction of TCNE with Cl- (and F-) anions (which are better nucleophiles in the aprotic solvents) led to the formation of 1,1,2,3,3-pentacyanoprop-2-en-1-ide anions. Thermodynamics, UV-Vis spectra, and structures, as well as contributions of electrostatics, orbital interactions, and dispersion to the interaction energies in the complexes of TCNE with various anions were closely related to the characteristics of the corresponding associations with the aromatic and p-benzoquinone acceptors. This points out the general equivalence of the interactions in the anion- π complexes with different π -acceptors and the critical role of the nature of the anions in these bindings.

Received 27th June 2024, Accepted 19th July 2024

DOI: 10.1039/d4cp02573c

rsc.li/pccp

1. Introduction

Following seminal theoretical articles showing the attraction of anions to electron-deficient π -systems (e.g., triazine or perfluorobenzene) in 2002, $^{1-3}$ anion- π interactions became one of the central topics of supramolecular chemistry. 4-6 These computational works were followed by experimental verifications of anion- π binding⁷⁻¹¹ demonstration of its high potential for anion recognition and transport, catalysis, and other applications. 12-16 The detailed accounts of the development in this area is described in several excellent reviews. 5,6,11,12 The main attention in the studies of this counter-intuitive interaction was directed toward the bonding between anions and aromatic molecules with

electron-withdrawing substituents (e.g., halogens, nitro or cyano groups).1-6 There are also several publications describing the associations of anions with the faces of cyano- and/or halogensubstituted benzoquinones, and studies of attractive interaction of lone pairs with the π^* antibonding orbitals of carbonyl groups. 17-19 Nevertheless, the data about binding between anions and the simplest π-systems, molecules containing one C=C double bond, is scarce. 9,20,21 This raises the question about the nature and characteristics of such an unusual bonding, and its relation to previously described anion– π interactions.

Similarly to the aromatic and benzoquinone molecules, the possibility of the attraction of anions to alkenes depends on the presence of the electron-withdrawing substituents which decrease electron density over the face of the π -system. Thus, to explore the anion- π interaction involving such species, we turned to a well-known olefinic π -acceptor, tetracyanoethylene (TCNE, Fig. 1).22 The withdrawal of the electron density from the ethylene fragment by the four cyano-groups results in a positive electrostatic potential over the face of this essentially planar molecule (Fig. 1).21 This suggests an attraction of anions to this area. Indeed, the crystallographic literature contains X-ray structures of associations of TCNE with bromide, thiocyanate, and tetrahalometallates. 9,20,21 Yet, there are essentially

^a Department of Chemistry, Ball State University, Muncie, Indiana 47306, USA. E-mail: svrosokha@bsu.edu

^b Department of Chemistry, Purdue University, West Lafayette, Indiana 47907, USA † Electronic supplementary information (ESI) available: X-Ray structures and details of the X-ray crystallographic analysis, results of the UV-Vis measurements and details of the treatment of the spectral data, quantum theory of atoms in molecules and energy decomposition analyses data, energies and atomic coordinates of the optimized complexes. CCDC 2353176-2353181. For ESI and crystallographic data in CIF or other electronic format see DOI: https://doi.org/10.1039/ d4cp02573c

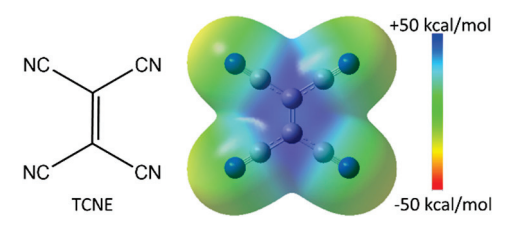


Fig. 1 Structure, acronym and surface electrostatic potential of TCNE (at 0.001 a.u. electron density).

no experimental or computational data on the thermodynamics and spectral properties of these complexes in solutions, about the bonding of TCNE with other anions, or the nature and main components of this bonding interaction.

In the current work, we examined the interaction of TCNE with various anions in the solid state and solutions, as well as scrutinized their properties using computational methods. Our goal was to compare anion– π complexes of olefinic π -acceptors with those involving aromatic (e.g., tetracyanopyrazine) or p-benzoquinone (e.g., tetrafluoro-p-benzoquinone) acceptors, and to clarify similarities and distinctions (if any) in the characteristics of the different types of complexes.

Besides the π -acceptors, characteristics of the anion- π complexes are determined by the nature of the anions. We have shown earlier that while the overall strength of interaction is similar, the contributions of the electrostatics, dispersion, and orbital interactions were very different for complexes of aromatic or p-benzoquinone acceptors with polyatomic fluoro- or oxoanions as compared to those with monoatomic halide anions.²³ These distinctions manifested in different experimental UV-Vis spectral properties of the complexes. Thus, to verify the generality of these observations, we examined herein interaction of TCNE with anions with different structural and electronic characteristics. They include monoatomic (halides), linear (thiocyanate), planar (NO₃⁻), tetrahedral (BF₄⁻ and ClO₄⁻), and octahedral (PF₆⁻) species. Besides, these anions allow to compare properties of complexes with nucleophilic (and reducing) species with those of inert weakly-coordinating and difficult to oxidize oxo- and fluoroanions.

Indeed, many electron-rich anionic species, in particular halides, are good reducing agents and nucleophiles. On the other hand, the presence of four cyano-substituents makes TCNE molecule a strong π -acceptor with a reduction potential of 0.17 V vs. SCE in acetonitrile.²⁴ As such, it might be easily reduced by various chemical or electrochemical methods. In fact, the reaction of TCNE with iodide was one of the earliest and the most common methods of preparation of the anionradicals of this π -acceptor. ^{25–27} These persistent anion-radicals played a central role in the development of the molecular magnets and the concept of multicenter (pancake) bonding.²⁸ Also, the interaction of TCNE with various nucleophiles in the presence of water resulted in the formation of polycyanosubstituted anionic species. 29,30 The σ -bonded complexes of anions with TCNE were suggested as the intermediates of these transformations.³⁰ As such, another goal of the current work was to establish boundaries between the reversible formation

of the anion- π complexes with TCNE and the irreversible chemical processes, in particular 1e-reduction or nucleophilic addition, of this π -acceptor.

Results and discussion

2.1. X-Ray crystallography of the anion- π associations and products of reactions of TCNE with anions

Co-crystallization of TCNE with $(Pr_4N)NO_3$ produced 1D stacks of alternating π -acceptor and anion moieties (Fig. 2A). Within these stacks (which are surrounded by the tetrapropylammonium counter-ions), NO_3^- anions were nested between two TCNE molecules. The latter are tilted relative to each other by about 65°, but every other TCNE moiety is parallel (similar to the observed earlier for anion- π bonded stacks with aromatic tetracyanopyrazine acceptors).²⁰

Co-crystals of TCNE with methyltriphenylphosphonium bromide, (MePh₃P)Br, comprised analogous alternating chains of TCNE and anions (Fig. 2B). The bromide anions were located close to the top of the sp² carbons, with Br–C=C angles of 111.7 and 83.0 deg. Both TCNE/NO₃⁻ and TCNE/Br⁻ chains comprise multiple contacts between anions and π -acceptors which are shorter than the sums of the van der Waals radii of the corresponding atoms. Selected interatomic distances in these co-crystals are listed in Table 1.

Co-crystallization of TCNE with tetrapropylammonium perchlorate or tetrafluoroborate salts produced 1:2 solid-state complexes in which two anions are arranged on both sides of the $\pi\text{-acceptors}$ (Fig. 2C and Fig. S1 in the ESI,† note that similar arrangements are observed for ((Pr_4N)PF_6)_2·TCNE, but ions and TCNE moieties are disordered in these co-crystals). While stoichiometry and the architectures of these co-crystals are different from those formed by TCNE with Br $^-$ or NO $_3$ $^-$, they share the same principal feature. Specifically, the anions are located over the faces of the TCNE molecules, and they show multiple contacts that are shorter than the van der Waals separations (Table 1). This indicates a strong attraction of

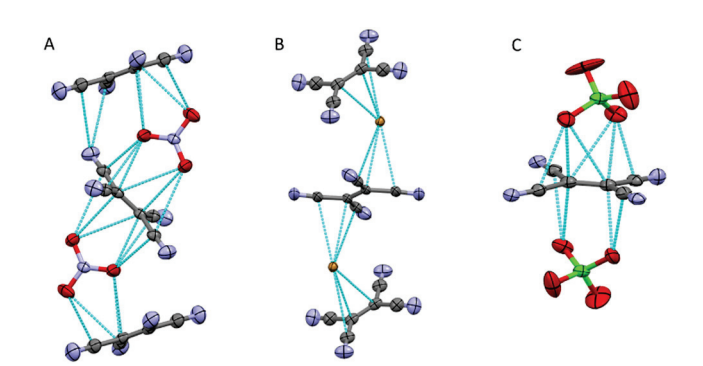


Fig. 2 Fragments of the crystal structures showing chains of the alternating anions and π -acceptors in $(Pr_4N)NO_3$ -TCNE (A), $(MePh_3P)Br$ -TCNE (B), and the 2:1 complex of $((Pr_4N)ClO_4)_2$ -TCNE (C). Note that countercations are omitted for clarity. The blue lines show contacts shorter than the van der Waals separations of the interacting atoms (3.22 Å and 3.55 Å for C/O and C/Br pairs, respectively).

PCCP Paper

Table 1 Characteristics of the selected short contacts in the co-crystals of TCNF with various anion

Anion	Contact	d _{X···C} , Å	$\rho(\mathbf{r})$, a.u.	<i>H</i> (r), a.u.	$-\Delta E$, a kcal mol ⁻¹
NO ₃	O-C _{C=C}	2.713	0.0102	0.0021	2.1
	$O-C_{C \equiv N}$	2.813	0.0090	0.0017	1.8
Br^{-}	$Br-C_{C=-C}$	3.343	0.0109	0.0008	1.9
	$Br-C_{C=-C}$	3.350	0.0103	0.0009	1.7
ClO_4^-	$O-C_{C \equiv N}$	2.798	0.0122	0.0018	2.6
	$O-C_{C=C}$	2.860	0.0111	0.0016	2.1
$\mathrm{BF_4}^-$	$O-C_{C=C}$	2.841	0.0160	0.0021	3.5
	$O-C_{C\equiv N}$	2.902	0.0070	0.0012	1.2

^a Calculated based on the energy density, $E = 1/2V(\mathbf{r})$. ³¹

anions to the π -acceptor. To verify this suggestion, we carried out OTAIM and NCI analyses of these solid-state associations.

A quantum theory of atoms in molecules (QTAIM) analysis³² revealed bond paths between anions and TCNE in each solidstate association (Fig. 3 and Fig. S2 in the ESI†).

Characteristics of the (3, -1) bond critical points (BCPs) along these bond paths are listed in Table 1 and Table S1 in the ESI.† The electron densities at BCPs for all associations are close to 0.01 a.u. These values are typical for moderately strong noncovalent interactions.³³ The very small positive values of energy density at these points indicate a predominantly electrostatic nature of these bondings. The energies of these interactions (estimated using values of the potential energy density at BCPs³¹) were around 2 kcal mol^{-1} . The NCI analysis³⁴ showed blue-green areas around each BCP which further confirmed a relatively weak attractive interaction between anions and TCNE.

While the interaction of TCNE with salts of fluoro-/oxoanions, and bromide led to the formation of anion- π associations, crystallization with alkylammonium chloride or fluoride salts produced 1,1,2,3,3-pentacyanoprop-2-en-1-ide (abbreviated hereinafter as PCP⁻) anions (Fig. S3 in the ESI†).‡ Also, reactions of TCNE with alkylammonium salts of iodide resulted previously in the reduction of TCNE and crystallization of the salts of TCNE^{-•} anion-radicals.²⁶ Thus, besides the well-known reduction of TCNE by iodide (due to the low redox potentials for the I_3^-/I^- pair of 0.06 V vs. SCE³⁵) the formation of the persistent anion- π complexes of TCNE with halides is limited by the nucleophilicity of anions (since chloride and fluoride are better nucleophiles in aprotic solvents as compared to the

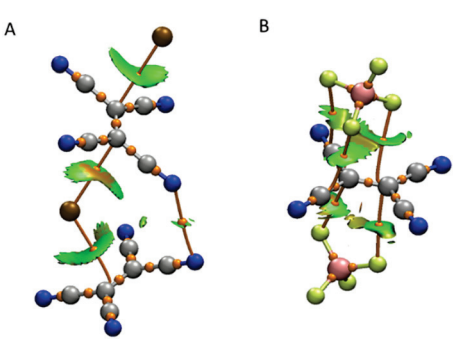


Fig. 3 QTAIM and NCI analyses of the solid-state (MePh₃P)Br·TCNE (A) and ((Pr₄N)BF₄)₂·TCNE (B) associations (using atomic coordinates extracted from the X-ray structures). Orange lines and orange spheres show bond paths and BCPs and blue-green areas indicate bonding interactions (note that calculations were done using dianinic fragments shown in this figure).

bromide³⁶). To further elucidate the interactions between TCNE and various anions, we turned to their measurements of their properties in solution.

2.2. UV-Vis study of the interaction of anions with TCNE

The addition of Br anions to the solutions of TCNE in acetonitrile or dichloromethane led to the appearance of a new absorption band in the UV-Vis spectra (with λ_{max} at 469 nm and 460 nm in CH₂Cl₂ and CH₃CN, respectively) which was not present in the spectra of the individual reactants (Fig. 4 and Fig. S4 in the ESI†). In solutions with a constant concentration of TCNE, the intensity of this band increased with the rise of the concentration of Br anions. This dependence was well-fit to the binding isotherm of a 1:1 complex between TCNE and Br-:

$$TCNE + Br^- \rightleftharpoons [TCNE \cdot Br^-]$$
 (1)

In contrast to Br⁻, an addition of I⁻ or Cl⁻ anions to the solutions of TCNE resulted only in transient formation of anion- π complexes. In particular, the spectrum of the solution obtained upon the addition of the iodide to the solution of TCNE in dichloromethane at 20 °C resulted in immediate formation of a spectrum that represented a superposition of the absorption of TCNE^{-•} anion-radical (band at 425 nm with the characteristic vibrational splitting²⁷) and I₃⁻ anions (strong band with a maxima at 360 and 295 nm (ref. 17)). This indicates the fast reduction of TCNE by iodide with formation of TCNE -• and I₃⁻ (this reaction is a common method of preparation of TCNE anion-radicals.²⁵⁻²⁷) However, when the solutions of TCNE and I were mixed at -85 °C, a broad absorption band appeared at 650 nm (Fig. 5). DFT calculations§ and Mulliken correlations (vide infra) indicated that this band represents absorption of a TCNE·I⁻ complex. Warming of this solution led to fast decrease of the disappearance of this band and

[‡] The PCP anions were previously synthesized by the reaction of TCNE with water in the presence of a base (which formed a σ-bonded intermediate with the π -acceptor). ^{29,30} Also, computational analyses in the previous studies ¹⁷ and in the current work indicated that $\mbox{\ensuremath{F^{-}}}$ anions form the $\sigma\mbox{-bonded}$ intermediates with the π -acceptors which explains the formation of PCP $^-$ in the presence of these nucleophilic anions. To the best of our knowledge, however, σ -complexes with Cl- anions were not reported and the computations of TCNE·Cl- pairs in the current work produced anion- π complexes as the most stable structure. Yet, the location of chloride in these complexes was well suited for the nucleophilic attack on the sp² carbon. Furthermore, while the Cl···C distance in such complexes optimized in CH2Cl2 was 2.694 Å, calculations in the gas phase produced association with the Cl···C distance of 2.142 Å (and the essentially tetrahedral geometry of the carbon). The detailed analysis of the mechanism of the formation of PCP- requires, however, a separate study and it is beyond the scope of the current work, which is focused on the nature of the anion- π complexes of TCNE with various anions.

[§] The energies of the absorption bands obtained from the TD DFT calculations were 3.18 eV, 2.68 eV, and 2.21 eV, for an ion- π complexes of TCNE with Cl⁻, Br⁻. and I anions, respectively (as compared to the measured values of 3.04 eV, 2.65 and 1.91 eV of the persistent or transient bands measured in the solution of TCNE with these anions). The calculated absorption band energy of PCP- anion was 3.54 eV as compared to the energy of 4.12 eV of the absorption band formed at λ = 301 nm upon the addition of chloride to the solution of TCNE.

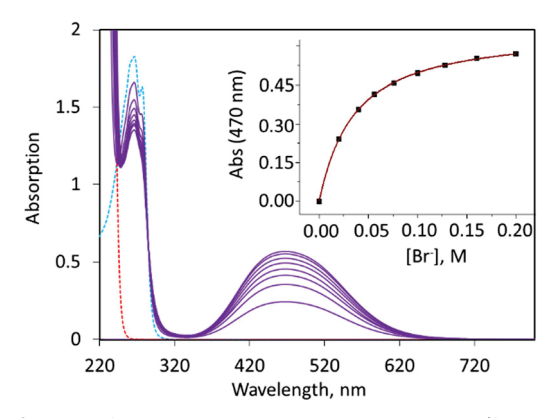


Fig. 4 Spectra of solutions with variable concentrations (from 0.02 to 0.2 M) of (Bu₄N)Br and a constant concentration (1.5 mM) of TCNE in CH₂Cl₂ (purple lines). Dashed red and blue lines show spectra of the solutions of individual (Pr₄N)Br and TCNE, respectively. Insert: Dependence of the intensity of absorption at 470 nm on the concentration of Br $^-$ (the solid line shows a fit of the data to a 1:1 binding isotherm).

appearance of the bands of TCNE^{\bullet} and I_3 ⁻. It suggests that the anion– π complex of TCNE with iodide represent an intermediate in the formation of TCNE^{\bullet} anion-radical, *i.e.*

$$2TCNE + 3I^- \rightleftharpoons 2[TCNE \cdot I^-] + I^- \rightarrow 2TCNE^{-\bullet} + I_3^-$$
 (2)

The addition of chloride to the solution of TCNE resulted in the appearance of a broad absorption band at 408 nm (Fig. 6). The intensity of this band decreased with time and a new absorption band with a maximum at 301 nm appeared (see time-dependent spectra in Fig. S5 in the ESI,† note that mixing of the solution of TCNE and Cl $^-$ in acetonitrile led to immediate appearance of the analogous band at 300 nm). TD DFT calculations of the TCNE Cl $^-$ (anion– π) complex§ and 1,1,2,3,3-pentacyanoprop-2-en-1-ide anions, PCP $^-$ (which were obtained in the crystalline state from the solutions containing TCNE and chloride) produced absorption bands which were reasonably close to the bands at 410 and 310 nm, respectively. It suggests

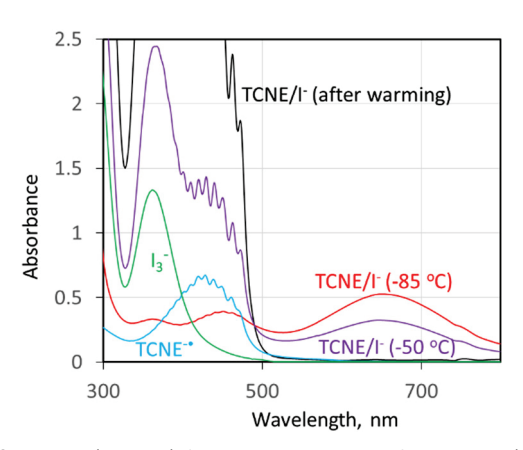


Fig. 5 Spectrum (red line) formed upon mixing of equimolar (1.0 mM) solutions of TCNE and (Bu₄N)I in CH₂Cl₂ at $-85\,^{\circ}\text{C}$. Violet and black lines show spectra measured upon warming of this solution to $-50\,^{\circ}\text{C}$ and to $+20\,^{\circ}\text{C}$. Blue and green lines show spectra of the individual TCNE $^{-\bullet}$ and I $_3^{-}$ ions, respectively.

that these bands represent anion– π complex and PCP⁻ anions. Furthermore, the absorption band energies of the complexes of TCNE with halides (and with thiocyanate²¹) follow the same Mulliken correlation³⁷ with the difference of the redox-potentials of the interacting species (Fig. 7) as the reported earlier bands of the halides and thiocyanate complexes with aromatic and benzoquinone acceptors.^{17,21} This supports assignments of the transient absorption bands measured with I⁻ and Cl⁻ anions and suggests a close relationship between complexes with different π -acceptors.

In contrast to halides, addition of oxo- or fluoroanions to the solutions of TCNE did not produce new absorption bands in the UV-Vis range (Fig. 8 and Fig. S6 in the ESI†). The close inspections of the spectra of these solutions revealed, however, that their absorptions deviate from that of TCNE itself. Subtraction of the latter from the spectra of mixtures showed that the addition of the oxo- or fluoroanions results in a small increase or decrease of the absorption in various regions of the TCNE band. Importantly, these differential absorptions could be fitted with 1:1 binding isotherms (Fig. S6–S9 in the ESI†) similar to those used for fitting of the spectra in solutions with bromide.

The values of the apparent equilibria constants K of 8 M^{-1} to 80 M⁻¹ which were obtained from such fittings of the UV-Vis data measured in dichloromethane are listed in Table S3 in the ESI.† For comparison, Table S3 (ESI†) includes also the characteristics of the related anion- π complexes with the aromatic tetracyanopyrazine (TCP), tetrafluoro- (pFA) or dichlorodicyanop-benzoquinone (DDQ) π -acceptors which were reported earlier.²³ It should be stressed that due to the variation of ionic strength in the series of the solutions that were used for the UV-Vis measurements, the values of K do not represent true equilibrium constants.³⁸ Still, the fact that the values obtained for the complexes of TCNE are in the same range as those measured in an analogous way with aromatic and p-benzoquinone molecules indicates a comparable strength of the interaction with different types of π -acceptors. Also, in agreement with the calculated solvent dependence of the binding energies (Fig. S10 and Table S4 in the ESI†) and our previous studies of complexes with p-benzoquinones, 23 the apparent constant of the formation of the complex of TCNE with Br⁻ measured in acetonitrile (7.0 M⁻¹) was lower than that in dichloromethane (31 M⁻¹). The spectral changes occurring upon the addition of ${\rm PF_6}^-$, ${\rm BF_4}^-$, and ${\rm ClO_4}^-$ to TCNE in acetonitrile were too small for measurements of formation constants of the corresponding complexes in this solvent.

Overall, UV-Vis measurements showed that the spectral features and apparent formation constants of the complexes of TCNE with various types of anions are similar to those reported earlier for the analogous associations with the aromatic and p-benzoquinone π -acceptors. ²³ To examine the nature of the anion- π interactions in the complexes with TCNE, we turned to computational analyses.

2.3. Computational analysis of the interaction of TCNE with anions

The structures resulting from M06-2X/def2-TZVPP optimization of the complexes of TCNE with various anions together with the

PCCP Paper

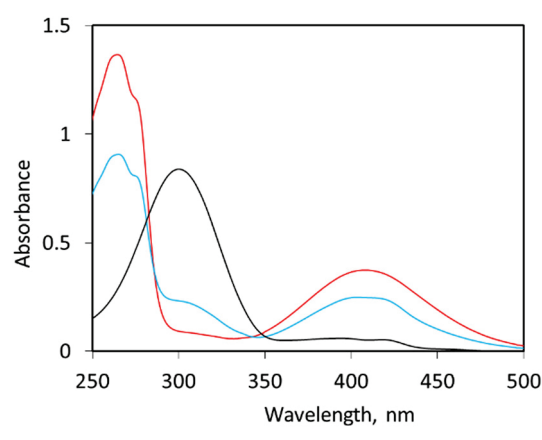


Fig. 6 Spectra of the solutions containing TCNE and Bu₄NCl in dichloromethane measured at 22 °C immediately after mixing (red line showing band of anion- π complex at 410 nm), after 10 min (blue line), and after 24 h (black line showing band of PCP- at 310 nm).

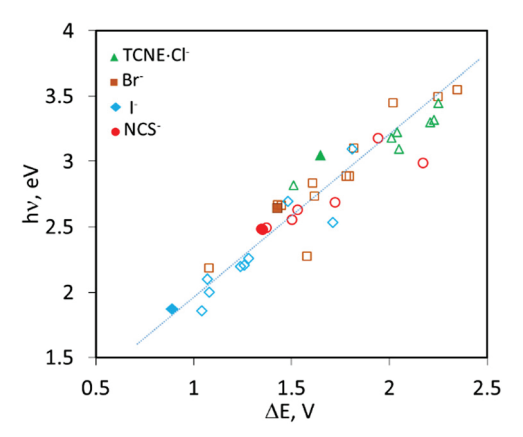


Fig. 7 Correlation between energies of the absorption bands and the difference of the redox potentials of the reactants in the complexes of Cl-(green triangles), $\rm Br^-$ (brown square), $\rm I^-$ (blue rhombuses), and NCS $^-$ (red circles) with different π -acceptors. The filled symbols indicate complexes with TCNE, and open symbols present the data with aromatic and p-benzoquinone π -acceptors 17 (see Table S2 in the ESI \dagger for the details).

results of their QTAIM and NCI analyses are illustrated in Fig. 9. In general, the arrangements of the anions and π -acceptors in the optimized 1:1 complexes were consistent with the structures of the solid-state associations obtained from the X-ray crystallographic analysis (although the latter represented 1D chains with 2:2 anion- π -acceptor contacts or 2:1 complexes). In particular, oxo- and fluoroanions in these complexes were located over the C=C double bond. The calculated complex with nitrate, however, comprised essentially co-planar NO₃ and TCNE moieties (while the NO₃⁻ plane is close to perpendicular to the TCNE molecules and shows close O···C contacts on both its sides in the X-ray structure). All these complexes show contacts between the anions and TCNE which are shorter than their van der Waals separations (Table 2), and these interatomic distances are consistent with the values measured in the solid-state.

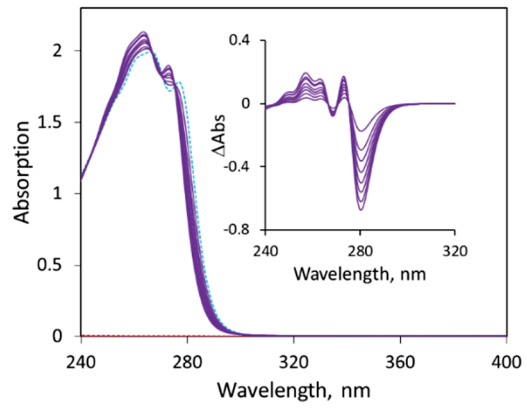


Fig. 8 Spectra of the solutions (purple lines) containing variable (20 to 200 mM) concentrations of (Bu₄N)BF₄ and a constant (1.5 mM) concentration of TCNE in CH₂Cl₂. Dashed red and blue lines show spectra of the individual solutions of (Pr₄N)BF₄ and TCNE, respectively. Insert: Differential spectra of the solution which were obtained by the subtraction of the absorption of individual components from the absorption of the mixture.

Optimizations of the complexes of TCNE with Cl⁻, Br⁻ and I anions produced structures similar to those obtained by X-ray analysis for the complex of TCNE with bromide. It should be noted, however, that the Br. . . C separation in the optimized complex is about 0.4 Å shorter than in the experimental X-ray structure in Table 1. Such a difference is probably related to the fact that the solid-state associations represent 1D chains in which each bromide interacts with two TCNE molecules and vice versa, as well as stronger effects of counter-ions and crystals forces on the location of these monoatomic anions. The halide anions were located near the top of one of the sp² carbons. The X-C=C angles (109.2, 108.1 and 107.2° for optimized pairs with Cl⁻, Br⁻, and I⁻, respectively) are close to the value characteristic for the Burgi-Dunitz trajectory for the nucleophilic attack on an sp² carbon.³⁹ In comparison, the optimizations of the systems with the stronger nucleophiles, F⁻ and N₃⁻ (the latter was chosen for the comparison with NCS $^-$) produced σ -bonded

The binding energies of the anion to TCNE in all calculated anion- π complexes are in the 9 \pm 3 kcal mol⁻¹ range. Similar values were reported earlier for the complexes of the same anions with aromatic and p-benzoquinone acceptors.²³ The binding of anions in the σ-bonded complexes with F⁻ and N₃⁻ are about three times stronger.

The QTAIM analysis showed bond paths and BCPs between anions and TCNE moieties in all calculated complexes. The energy and electron densities at BCPs (Table S5 in the ESI†) are similar to those in the experimental solid-state associations.

While the binding energies for the oxo- and fluoroanions were similar to those in the anion- π complexes with (pseudo-)halides, the spectral properties of these complexes obtained via TD DFT calculations were different. The optimized anion- π complexes with (pseudo-)halides show intense absorption bands in the visible range. Their energies are close to those measured experimentally, and they decrease with the increase of electron-donor abilities of the anions, which supported the

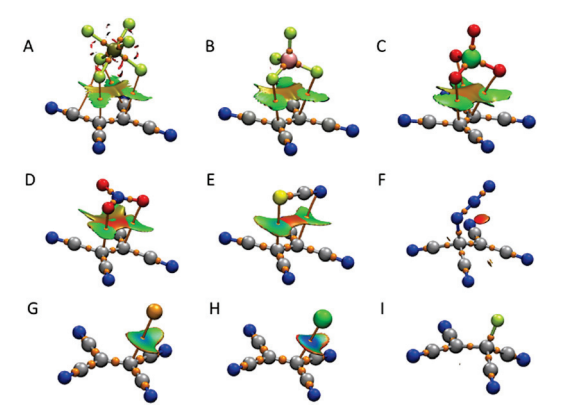


Fig. 9 Superposition of the results of QTAIM and NCI analyses onto the optimized structures of the complexes of TCNE with PF_6^- (A), BF_4^- (B), ClO_4^- (C) NO_3^- (D), NCS^- (E) N_3^- (F), Br^- (G), Cl^- (H) and F^- (I). The bond paths and critical (3, -1) points (from QTAIM) are shown as orange lines and spheres, and blue-green areas (from NCI) indicate bonding interactions.

charge-transfer character of these transitions (the computational analysis showed that they represent a photoinduced transfer of electrons from the highest occupied molecular orbitals, HOMOs, of the complex which were located primarily on the anions to the lowest unoccupied molecular orbitals, LUMOs, which resides mainly on TCNE). In comparison, the absorption bands in the calculated spectra of complexes with oxo- and fluoroanions are close to those of the individual TCNE acceptors. Since oxo- and fluoroanions are poor electron donors (*i.e.*, their HOMOs are lower), the electronic transitions from the HOMOs (residing on the anions) to the LUMOs located on TCNEs overlap with the intramolecular transitions within the individual π -acceptors.

Besides the differences in the spectra, the better electron-donating properties of the (pseudo-)halide anions explain the higher ground-state $n-\pi^*$ charge transfer from these anions to TCNE in their anion- π complexes as compared to the value found in the complexes with the oxo- and fluoroanions (Table 2). The $n-\pi^*$ charge transfer led to slight (about 0.007 Å) lengthening of the C—C bond (Table 2) as compared to the bond (1.345 Å) in the optimized individual TCNE and it suggests the higher contribution of charge-transfer (molecular-orbital) interactions in the complexes with the halides.

Table 2 Characteristics of the optimized anion $-\pi$ complexes

\mathbf{X}^{-}	ΔE , kcal mol ⁻¹	$d_{ ext{X}\cdots ext{C}}$, $\overset{a}{ ext{A}}$	λ_{max} , nm	Δq , e	$d_{\mathrm{C=-C}}$, Å
PF ₆	-7.3	2.780	262	0.02	1.346
$\mathrm{BF_4}^-$	-8.4	2.754	262	0.02	1.346
ClO_4^-	-8.5	2.852	287	0.03	1.347
NO_3^-	-9.8	2.730	301	0.08	1.349
Cl^-	-9.7	2.694	390	0.20	1.357
Br^{-}	-7.9	2.957	461	0.16	1.355
I^-	-6.6	3.202	560	0.17	1.355
NCS^-	-11.8	2.841	448	0.22	1.357
N_3^-	-24.5	1.529	293	0.88	1.490
\mathbf{F}^{-}	-37.6	1.418	230	0.65	1.465
NCS ⁻ N ₃ ⁻	-11.8 -24.5	2.841 1.529	448 293	0.22 0.88	1.357 1.490

 $[^]a$ The shortest contact between the anion and TCNE. b Charge-transfer from the anion to the TCNE moiety. c The C—C bond length.

To verify the distinctions in the interactions of TCNE with different anions, we performed an energy decomposition analysis (EDA) of these bondings using the AMS suite of programs. ⁴⁰ This method decomposes the intermolecular interaction energy into electrostatic, $\Delta E_{\rm elstat}$, Pauli repulsion, $\Delta E_{\rm Pauli}$, orbital (charge-transfer) interaction, $\Delta E_{\rm oi}$ and dispersion, $\Delta E_{\rm disp}$, components: ⁴¹

$$E_{\text{int}} = E_{\text{elstat}} + E_{\text{Pauli}} + E_{\text{oi}} + E_{\text{disp}}$$
 (3)

All these values are listed in Table S6 in the ESI.† Notably, while binding energies, ΔE , are rather close for all anion– π bonded complexes, the values of $E_{\rm elstat}$, $\Delta E_{\rm oi}$, and $\Delta E_{\rm disp}$ depend substantially on the nature of the anions. Variations of the contributions (in %) of these components to the attractive interaction (e.g., $\Delta E_{\rm elstat}/(\Delta E_{\rm elstat} + \Delta E_{\rm oi} + \Delta E_{\rm disp}) \times 100\%$) are illustrated in Fig. 10.

The data in Fig. 10 show that electrostatics represents the most significant component of attractive interaction energy in all anion– π complexes. Contributions of dispersion are more than three times lower than those of electrostatics. The contributions of both $\Delta E_{\rm elstat}$ and $\Delta E_{\rm disp}$ are lower in the complexes with (pseudo-)halides as compared to that with the oxo- and fluoro-anions. Accordingly, orbital interactions are much stronger in the complexes with (pseudo-)halides than in the complexes with oxo- and fluoroanions. The $E_{\rm oi}$ values are approaching $E_{\rm ES}$ in the anion– π complexes with (pseudo)halides, and the contributions of different components in these associations are comparable to those in the σ -bonded complexes formed by TCNE with N_3^- and F^- anions. The substantial contribution of the molecular-orbital interaction explains the appearance of the intense charge-transfer absorption bands in the anion– π complexes with (pseudo-)halide anions. 42

Methods

3.1. Materials

Commercially available TCNE was purified by sublimation, and tetrabutyl- or tetrapropylammonium salts of tetrafluoroborate, thiocyanate, perchlorate, hexafluorophosphate, and halides were purified by recrystallization. The methyltriphenylphosphonium salt of bromide, (MePh $_3$ P)Br, was used for the preparation of single crystals without purification. Tetrapropylammonium salts of nitrate and hexafluorophosphate were prepared by neutralization of the corresponding acid with a solution of tetrapropylammonium hydroxide followed by the recrystallization from dichloromethane/hexane mixtures. Dichloromethane and acetonitrile were distilled over P_2O_5 under an argon atmosphere before use.

3.2. X-Ray crystallography

Single crystals of $(Pr_4N)NO_3$ ·TCNE, $(Pr_4N)PF_6$ ·TCNE, $((Pr_4N)-ClO_4)_2$ ·TCNE, and $(Pr_4N)BF_4$ ·TCNE, were prepared by cooling acetonitrile solutions containing equimolar (0.2 mmol each) quantities of TCNE and the corresponding salt from room temperature to -30 °C and keeping solutions at this temperature for several days. Single crystals obtained by similar procedures with tetrabutyl- or tetrapropylammonium salts of F^- or Cl^- anions comprised 1,1,2,3,3-pentacyanoprop-2-en-1-ide (PCP^-)

PCCP Paper

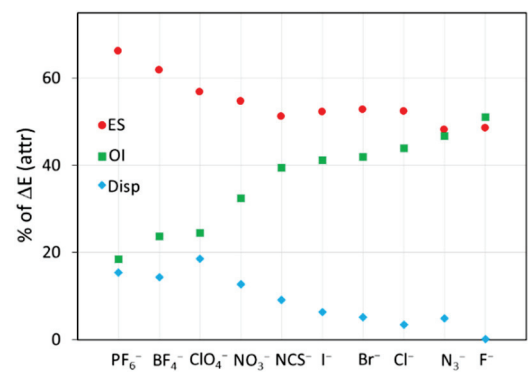


Fig. 10 Contributions (in %) of $\Delta E_{\rm elstat}$ (red circles), $\Delta E_{\rm oi}$ (green squares), and $\Delta E_{\rm disp}$ (blue rhombus) to the attractive interactions in the complexes of TCNE with various anions.

salts, (Bu₄N)PCP (Fig. S3, ESI†) or (Pr₄N)PCP. To prepare crystals of (MePh₃N)Br·TCNE, the equimolar (1.0 mmol) amounts of (MePh₃N)Br and TCNE were stirred for several minutes in 3 mL of a 10:1 mixture of dichloromethane and hexane. The undissolved solid was filtered off and the solution was cooled to -30 °C. Red crystals of (MePh₃N)Br·TCNE formed after several days.

The X-ray measurements were carried out on a Bruker AXS D8 Quest diffractometer with a molybdenum radiation X-ray tube ($\lambda=0.71073$ Å). Reflections were indexed and processed, and the files were scaled and corrected for absorption using APEX4.⁴³ The space groups were assigned using XPREP within the SHELXTL suite of programs, the structures were solved by dual methods using using ShelXT and refined by full-matrix least-squares against F^2 with all reflections using Shelxl2019 with the graphical interface Shelxle.^{44–46} Crystallographic, data collection, and structure refinement details are listed in Table S7 in the ESI.† Complete crystallographic data, in CIF format, have been deposited with the Cambridge Crystallographic Data Centre. CCDC 2353176–2353181 contain the supplementary crystallographic data for this paper.†

3.3. UV-Vis measurements

The formation of complexes between TCNE and various anions was studied at 22 °C via UV-Vis measurements of a series of solutions with a constant (2-10 mM) concentration of TCNE and variable concentrations (from 0 to 0.4 M) of anions. A Dewar equipped with a quartz lens was used for the measurements at -85 °C. The apparent formation constants, K, were obtained (see the ESI† for details) via regression analysis of the differential intensities of absorption, ΔAbs (obtained by the subtraction of absorption of components from the absorption of their mixtures), for these series as described earlier. ^{17,23} Each point in these series represents a result of a separate measurement taken within 1-2 minutes after mixing solutions of TCNE and the salt of anion. In the case of the complexes of ClO₄, PF₆⁻, and BF₄⁻ anions, the spectra of the solutions remained constant for several hours (Fig. S10 in the ESI†). The spectra of the dichloromethane solutions of the complexes with bromide remained essentially constant for about 10-15 minutes, but small spectral changes were noticeable when such solutions were kept for several hours at room temperature (Fig. S11 in the ESI†). These changes suggest that very slow formation of the products of nucleophilic attack (similar to that in the systems with Cl $^-$) and/or redox processes in solutions of TCNE with Br $^-$ anions \P (note that similar time-dependent spectral changes were observed in dichloromethane solutions of TCNE and NCS $^-$ and NO3 $^-$ and the rates of these processes were higher in more polar acetonitrile). The analysis of the kinetics and mechanism of these reaction requires a separate study and is beyond a scope of the current work.

In the absence of hydrogen substituents in TCNE and anions, complex formation in solutions could be measured by ^{13}C NMR. However, such measurements require a higher concentration of TCNE, than that we used for the UV-Vis measurements. Due to the limited solubility of TCNE in dichloromethane, we used more polar deuterated acetonitrile, in which formation constants of the anion– π complexes are lower. 38 Under these conditions, we observed only very small shift of the signals of C—C and C \equiv N carbons in the spectra of anion– π complexes as compared to the individual TCNE (Fig. S12 in the ESI†). The measurements were further complicated by the substantial broadening of these signals in the presence of anions (up to their complete disappearance in the presence of bromide) which hindered quantitative measurements of complex formation using this method.

3.4. Computations

Geometries of the complexes were optimized without constraints via M06-2X/def2-TZVPP calculations (with ultrafinegrid option) using the Gaussian 09 suite of programs. 47-49 The absence of imaginary frequencies confirmed that the optimized structures represent true minima. Calculations with dichloromethane as the medium were done using a polarizable continuum model.⁵⁰ An earlier analysis demonstrated that intermolecular associations are well-modelled using this method. 17,38,51,52 The def2-TZVPP basis set does not include a diffuse function since previous analysis demonstrated that very similar results were obtained in the modelling of noncovalent interactions involving anions with the triple- ζ basis sets with and without diffuse functions.⁵³ Binding energies, ΔE were determined as: $\Delta E_{\rm b} = E_{\rm C} - (E_{\rm A} + E_{\rm X})$, where $E_{\rm C}$, $E_{\rm A}$, and $E_{\rm X}$ are sums of the electronic energy and zero-point energy (ZPE) of the optimized complex, TCNE and anion, respectively. The energies of the optimized complexes and their components are listed in Table S8 in the ESI.† The UV-Vis spectra were

 \P Note that anion- π complexes of TCNE with Br⁻, NCS⁻ and NO₃⁻ anions were sufficiently persistent for the measurements of the complex formation in solutions and for the preparation of their single crystal for the X-ray structural measurements (see Methods for details). However while these crystalline anion- π associations could be stored for several weeks in the refrigerator, the decomposition of the anion- π complexes of TCNE with these anions was observed in solution at room temperature (see Fig. S10 in the ESI.† Spectral changes suggest that these reactions led to formation of small amount of anion-radial of TCNE and/or PCP⁻ and these processes were faster in more polar acetonitrile than in dichloromethane. However, the detailed analysis of kinetics and mechanism of these processes requires a separate study and is beyond the scope of the current work.

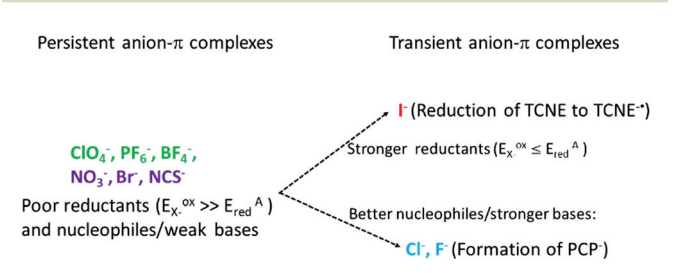
obtained *via* TD-DFT calculations of the complexes and their components optimized in the corresponding solvent. QTAIM³² and NCI³⁴ analyses of the solid-state associations and optimized complexes were performed using the atomic coordinates extracted from the X-ray structures with Multiwfn and visualized using VMD programs.^{54,55} The NCI setting was: isovalue = 0.5, color-coded with $sgn(\lambda 2)\rho$ in the range from -0.04 a.u. (blue, strong attractive interaction) to 0.02 a.u. (red, strong nonbonded overlap). Energy decomposition analyses (EDA) were carried out using the Amsterdam density functional (ADF) of the Amsterdam modelling suite ^{40,41} *via* single-point calculations with the B3LYP-D3 functional (since it allowed evaluation of the dispersion component of the interaction energy) and the TZ2P basis set available in AMS using atomic coordinates of the complexes optimized as described above.

4. Conclusions

The positive electrostatic potential over the face of TCNE suggests that anions are attracted to this π -acceptor. However, whereas the interaction of TCNE with non-coordinating inert anions ClO_4^- , BF_4^- , and PF_6^- led to formations of the persistent anion– π complexes, the kinetic stability of the other anion– π associations under study were delimited by the oxidation potentials and nucleophilicity of the anions (Scheme 1).

In particular, the values of E° for X^{\bullet}/X^{-} pair of 3.06, 2.03, 1.60 and 1.06 V νs . SCE for X = F, Cl, Br and I, respectively, are higher than that for TCNE/TCNE $^{\bullet}$ ($E^{\circ} = 0.17$ V). The redoxpotentials for the I_3^{-}/I^{-} pair, however, is 0.06 V, which explains facile reduction of TCNE to TCNE $^{\bullet}$ by I (eqn (2)) and similar reduction of tetrahalosubstituted p-benzoquinones which we reported earlier. As such, the transient appearance of the anion- π complexes upon mixing TCNE with iodide is followed by the fast formation of the TCNE $^{\bullet}$ anion-radicals.

The oxidation potentials of the other anions considered in the current work are higher than that of reduction potential of TCNE. As such, they are not capable of efficient reduction of this π -acceptor. (For example, redox-potential of the Br₃⁻/Br⁻ pairs is 0.39 V vs. SCE. Thus, while bromide reduces dichlorodicyano-p-benzoquinone, DDQ (E=0.52 V for DDQ/DDQ $^{\bullet}$ -pair), ¹⁷ the rate of reduction of TCNE by this anion is very small, if any.) However, the basicity and nucleophilicity of halide anions in aprotic solvents is increasing from I $^-$ to Br, Cl $^-$ and F $^-$. ³⁶ The interaction of TCNE with better nucleophiles and stronger basis, e.g. Cl $^-$ or F $^-$, led to chemical transformations producing PCP $^-$ anions (similar to that described



Scheme 1 Persistent vs. transient anion $-\pi$ complexes of TCNE.¶

previously in solutions containing basis and water^{29,30}), and only transient anion– π complexes were observed in the solutions of TCNE and Cl⁻ anions. Thus, among halide anions, only bromide (which is weaker reducing agent as compared to iodide, and weaker base/nucleophile than chloride or fluoride) formed rather persistent anion– π associations with TCNE.¶

It is also important to note, that thermodynamics, UV-Vis spectral, and structural features of the anion- π complexes of TCNE are closely related to the corresponding complexes of analogous anions with aromatic (such as tetracyanopyrazine) and p-benzoquinone (such as tetrafluoro-p-benzoquinone) acceptors. Furthermore, energy-decomposition analysis demonstrated that variations of the contributions of E_{elstat} , ΔE_{oi} , and ΔE_{disp} in complexes of TCNE with various anions (and also distinctions in the spectral properties of the corresponding complexes) are similar to those which were found for the complexes of the same anions with aromatic and p-benzoquinone π -acceptors. This underlines the critical role of the nature of the anions in these bindings. It also points towards a general equivalence of the interactions of anions with TCNE with those established earlier with aromatic molecules and p-benzoquinones. As such, it extends a realm of the fascinating anion- π interactions from the systems involving electron deficient arenes and quinones to the alkene π -acceptors.

Overall, this work (i) established the facile formation of anion- π complexes with TCNE and the conditions of the interchange between the persistent associations and transient complexes leading to redox or nucleophilic addition reactions, and (ii) demonstrated that characteristics of such complexes of this olefinic π -acceptor are closely related to those of the reported electron-deficient aromatic and p-benzoquiuinone molecules.

Author contributions

Conceptualization and methodology, S. V. R.; X-ray analysis, M. Z., UV-Vis measurements and crystallization, F. E. O. and S. M.; computations, F. E. O. and S. V. R.; data curation, F. E. O., S. M., M. Z., S. V. R.; writing – original draft preparation, S. V. R.; writing – review and editing, F. E. O., S. M., M. Z., S. V. R.; visualization, supervision, project administration, funding acquisition, S. V. R. All authors have read and agreed to the published version of the manuscript.

Data availability

The data supporting this article have been included as part of the ESI.† Crystallographic data for $(Pr_4N)NO_3$ ·TCNE, $(Pr_4N)PF_6$ ·TCNE, $((Pr_4N)ClO_4)_2$ ·TCNE, $(Pr_4N)BF_4$ ·TCNE, and $(MePh_3N)Br$ ·TCNE and Bu_4NPCP (where PCP = 1,1,2,3,3-pentacyanoprop-2-en-1-ide) has been deposited at the Cambridge Crystallographic Data Centre under 2353176–2353181 and can be obtained free of charge via https://www.ccdc.cam.ac.uk/data_request/cif.

PCCP Paper

Conflicts of interest

There are no conflicts to declare.

Acknowledgements

We thank the National Science Foundation (grant CHE-2003603) for the financial support of this work. Calculations were done on Ball State University's beowulf cluster, which is supported by the National Science Foundation (MRI-1726017) and Ball State University. X-Ray measurements were supported by the National Science Foundation through the Major Research Instrumentation Program under Grant No. CHE 1625543 (funding for the single crystal X-ray diffractometer).

Notes and references

- D. Quinonero, C. Garau, C. Rotger, A. Frontera, P. Ballester,
 A. Costa and P. M. Deya, *Angew. Chem., Int. Ed.*, 2002, 41, 3389.
- 2 I. Alkorta, I. Rozas and J. Elguero, J. Am. Chem. Soc., 2002, 124, 8593.
- 3 M. Mascal, A. Armstrong and M. D. Bartberger, *J. Am. Chem. Soc.*, 2002, **124**, 6274.
- 4 (a) A. Frontera, P. Gamez, M. Mascal, T. J. Mooibroek and J. Reedijk, *Angew. Chem., Int. Ed.*, 2011, **50**, 9564; (b) A. Bauzá, T. J. Mooibroek and A. Frontera, *ChemPhysChem*, 2015, **16**, 2496.
- 5 B. L. Schottel, H. T. Chifotides and K. R. Dunbar, *Chem. Soc. Rev.*, 2008, 37, 68.
- 6 (a) M. Giese, M. Albrecht and K. Rissanen, Chem. Commun., 2016, 52, 1778; (b) M. Giese, M. Albrecht and K. Rissanen, Chem. Rev., 2015, 115, 8867; (c) S. V. Rosokha, Chem-PlusChem, 2023, 88, e202300350.
- 7 G. Gil-Ramírez, E. C. Escudero-Adán, J. Benet-Buchholz and P. Ballester, *Angew. Chem., Int. Ed.*, 2008, 47, 4114.
- 8 S. Demeshko, S. Dechert and F. Meyer, *J. Am. Chem. Soc.*, 2004, **126**, 4508.
- Y. S. Rosokha, S. V. Lindeman, S. V. Rosokha and J. K. Kochi, *Angew. Chem., Int. Ed.*, 2004, 43, 4650.
- (a) O. B. Berryman, V. S. Bryantsev, D. P. Stay, D. W. Johnson and B. P. Hay, *J. Am. Chem. Soc.*, 2007, 129, 48; (b) D.-X. Wang and M.-X. Wang, *J. Am. Chem. Soc.*, 2013, 135, 892.
- 11 P. Ballester, Acc. Chem. Res., 2013, 46, 874.
- 12 (a) D.-X. Wang and M.-X. Wang, Acc. Chem. Res., 2020, 53, 1364; (b) H. Wang, W. Wang and W. J. Jin, Chem. Rev., 2016, 116, 5072.
- 13 Y. Zhao, Y. Cotelle, L. Liu, J. López-Andarias, A. B. Bornhof, M. Akamatsu, N. Sakai and S. Matile, *Acc. Chem. Res.*, 2018, 51, 2255.
- 14 D. Quinonero, A. Frontera and P. M. Deya, Anion- π interactions in molecular recognition, in *Anion Coordination Chemistry*, ed. K. Bowman-James, A. Bianchi and E. Garcia-Espana, 2012, p. 321.
- 15 J. Mareda and S. Matile, Chem. Eur. J., 2009, 15, 28.
- 16 E. Kuzniak, J. Hooper, M. Srebro-Hooper, J. Kobytarczyk, M. Dziurka, B. Musielak, D. Pinkowicz, J. Raya, S. Fertay and R. A. Podgajny, *Inorg. Chem. Front.*, 2020, 7, 1851.

17 S. Kepler, M. Zeller and S. V. Rosokha, *J. Am. Chem. Soc.*, 2019, 141, 9338.

- 18 (a) K. Molčanov, G. Mali, J. Grdadolnik, J. Stare, V. Stilinović and B. Kojić-Prodić, *Cryst. Growth Des.*, 2018, 18, 5182;
 (b) V. Milasinovic, V. Vukovic, A. Krawczuk, K. Molcanov, C. Hennig and M. Bodensteiner, *IUCrJ*, 2023, 10, 156.
- 19 R. W. Newberry and R. T. Raines, Acc. Chem. Res., 2017, 50, 1838.
- 20 B. Han, J. J. Lu and J. K. Kochi, Cryst. Growth Des., 2008, 8, 1327.
- 21 J. Wilson, T. Maxson, I. Wright, M. Zeller and S. V. Rosokha, Dalton Trans., 2020, 49, 8734.
- 22 T. Cairns, R. Carboni, D. Coffman, V. Engelhardt, R. Heckert, E. Little, E. Mcgeer, B. Mckusick, W. Middleton, R. Scribner, C. Theobald and H. Winberg, J. Am. Chem. Soc., 1958, 80, 2775.
- 23 F. E. Odubo, M. Zeller and S. Rosokha, *J. Phys. Chem. A*, 2023, **127**, 5851.
- 24 S. V. Rosokha and J. K. Kochi, Acc. Chem. Res., 2008, 41, 641.
- 25 (a) O. Webster, W. Mahler and R. Benson, *J. Am. Chem. Soc.*, 1962, **84**, 3678; (b) D. N. Dhar, *Chem. Rev.*, 1967, **67**, 611.
- 26 (a) A. Zheludev, A. Grand, E. Ressouche, J. Schweizer, B. G. Morin, A. J. Epstein, D. A. Dixon and J. S. Miller, J. Am. Chem. Soc., 1994, 116, 7243; (b) J.-M. Lu, S. V. Rosokha and J. K. Kochi, J. Am. Chem. Soc., 2003, 125, 12161.
- 27 S. V. Rosokha, M. D. Newton, M. Head-Gordon and J. K. Kochi, *Chem. Phys.*, 2006, 324, 117.
- 28 (*a*) J. S. Miller and A. J. Epstein, *Chem. Commun.*, 1998, 1319; (*b*) J. S. Miller, *Chem. Eur. J.*, 2015, **21**, 9302.
- 29 W. Middleton, R. Heckert, E. Little and C. Krespan, *J. Am. Chem. Soc.*, 1958, **80**, 2783.
- 30 Z. Rappoport, J. Chem. Soc., 1963, 4498.
- 31 E. Espinosa, E. Molins and C. Lecomte, *Chem. Phys. Lett.*, 1998, **285**, 170.
- 32 R. F. W. Bader, Chem. Rev., 1991, 91, 893.
- 33 P. L. A. Popelier, The QTAIM perspective of chemical bonding, *The Chemical Bond*, John Wiley & Sons, Ltd, 2014, p. 271.
- 34 E. R. Johnson, S. Keinan, P. Mori-Sánchez, J. Contreras-García, A. J. Cohen and W. Yang, *J. Am. Chem. Soc.*, 2010, 132, 6498.
- 35 J. Datta, A. Bhattacharya and K. K. Kundu, *Bull. Chem. Soc. Jpn.*, 1988, **61**, 1735.
- 36 M. B. Smith, *March's Advanced Organic Chemistry: Reactions, Mechanisms, and Structure*, Wiley, Hobolken, New Jersey, 8th edn, 2020.
- 37 R. S. Mulliken and W. B. Person, *Molecular Complexes*, Wiley, New York, 1969.
- 38 D. Howe, J. Wilson and S. V. Rosokha, *J. Phys. Chem. A*, 2022, **126**, 4255.
- 39 (a) H. B. Burgi, *Inorg. Chem.*, 1973, 12, 2321; (b) H. B. Burgi,
 J. D. Dunitz, J. M. Lehn and G. Wipff, *Tetrahedron*, 1974,
 30, 1563; (c) H. B. Burgi, J. D. Dunitz and E. Shefter, *J. Am. Chem. Soc.*, 1973, 95, 5065.
- 40 E. J. Baerends, T. Ziegler, J. Autschbach, D. Bashford, A. Berger, A. Bérces, F. M. Bickelhaupt, C. Bo, P. L. de Boeij, P. M. Boerrigter, S. Borini, et al., ADF2012.01, SCM, Amsterdam, 2012.
- 41 (a) F. M. Bickelhaupt and E. J. Baerends, Kohn-Sham density functional theory: predicting and understanding chemistry, in

- Reviews in Computational Chemistry, John Wiley & Sons, Ltd, 2000, p. 1; (b) G. te Velde, F. M. Bickelhaupt, E. Baerends, C. Fonseca Guerra, S. J. A. van Gisbergen, J. G. Snijders and T. Ziegler, J. Comput. Chem., 2001, 22, 931.
- 42 E. V. Anslyn and D. A. Dougherty, Modern Physical Organic Chemistry, Univ. Sci. Books, Sausalito, California, 2006, p. 186.
- 43 Bruker Apex3 v2016.9-0, SAINT V8.37A, Bruker AXS Inc., Madison, WI, 2016.
- 44 (a) G. Sheldrick, SHELXTL suite of programs, Version 6.14, 2000-2003, Bruker AXS Inc., Madison, WI, 2003; (b) G. M. Sheldrick, Acta Crystallogr., Sect. A: Found. Crystallogr., 2008, 64, 112.
- 45 G. M. Sheldrick, Acta Crystallogr., Sect. A: Found. Adv., 2015,
- 46 C. Hübschle, G. Sheldrick and B. Dittrich, J. Appl. Crystallogr., 2011, 44, 1281.
- 47 M. J. Frisch, G. W. Trucks, H. B. Schlegel, G. E. Scuseria, M. A. Robb, J. R. Cheeseman, G. Scalmani, V. Barone, B. Mennucci, G. A. Petersson, H. Nakatsuji, M. Caricato, X. Li, H. P. Hratchian, A. F. Izmaylov, J. Bloino, G. Zheng, J. L. Sonnenberg, M. Hada, M. Ehara, K. Toyota, R. Fukuda, J. Hasegawa, M. Ishida, T. Nakajima, Y. Honda, O. Kitao, H. Nakai, T. Vreven, J. A. Montgomery, Jr., J. E. Peralta, F. Ogliaro, M. Bearpark, J. J. Heyd, E. Brothers, K. N. Kudin,
- R. Kobayashi, N. Staroverov, J. Normand, K. Raghavachari, A. Rendell, J. C. Burant, S. S. Iyengar, J. Tomasi, M. Cossi, N. Rega, J. M. Millam, M. Klene, J. E. Knox, J. B. Cross, V. Bakken, C. Adamo, J. Jaramillo, R. Gomperts, R. E. Stratmann, O. Yazyev, A. J. Austin, R. Cammi, C. Pomelli, J. W. Ochterski, R. L. Martin, K. Morokuma, V. G. Zakrzewski, G. A. Voth, P. Salvador, J. J. Dannenberg, S. Dapprich, A. D. Daniels, O. Farkas, J. B. Foresman, J. V. Ortiz, J. Cioslowski and D. J. Fox, Gaussian 09, Revision C.01, Gaussian, Inc., Wallingford CT,
- 48 Y. Zhao and D. G. Truhlar, Theor. Chem. Acc., 2008, 120,
- 49 F. Weigend and R. Ahlrichs, Phys. Chem. Chem. Phys., 2005, 7, 3297.
- 50 J. Tomasi, B. Mennucci and R. Cammi, Chem. Rev., 2005, **105**, 2999-3093.
- 51 Z. Zhu, Z. Xu and W. Zhu, J. Chem. Inf. Model., 2020, **60**, 2683.
- 52 K. Wang, J. Lv and J. Miao, Theor. Chem. Acc., 2015, 134, 5.
- 53 A. Bauzá, D. Quiñonero, P. M. Deyà and A. Frontera, J. Phys. Chem. A, 2013, 117, 2651.
- 54 T. Lu and F. Chen, J. Comput. Chem., 2012, 33, 580.
- 55 W. Humphrey, A. Dalke and K. Schulten, J. Mol. Graphics, 1996, 14, 33.